PROCEEDINGS, Twentieth Workshop on Geothermal Reservoir Engineering
Stanford University, Stanford, California, January 24-26 1995
SGP-TR-150

NUMERICAL MODELING OF BOILING DUE TO PRODUCTION IN A FRACTURED RESERVOIR AND ITS FIELD APPLICATION

Yusaku Yano and Tsuneo Ishido

Geological Survey of Japan
1-1-3 Higashi, Tsukuba
305 Japan

ABSTRACT

Numerical simulations were carried out to characterize the behaviors of fractured reservoirs under production which causes in-situ boiling. A radial flow model with a single production well, and a two-dimensional geothermal reservoir model with several production and injection wells were used to study the two-phase reservoir behavior. The behavior can be characterized mainly by the parameters such as the fracture spacing and matrix permeability. However, heterogeneous distribution of the steam saturation in the fracture and matrix regions brings about another complicated feature to problems of fractured two-phase reservoirs.

INTRODUCTION

"MINC" method (Pruess and Narasimhan, 1985) is usually used for numerical simulation of fractured reservoirs. Pritchett and Garg (1990) made a classification of numerical treatments for fractured reservoirs, based on a spherical, zero-dimensional MINC model. In the classification, the time required for pressure equilibrium to be reached between the fracture zone and the matrix block (τ_{pe}), and the time required for temperature equilibrium to be reached due to heat conduction acting alone (τ_{hc}) are the basic parameters for choosing a suitable numerical treatment including MINC method and porous medium assumption.

If τ_{pe} is short enough compared with the time of interest, the pressures within the rock matrix is in equilibrium with fracture zone. In this case, porous medium assumption can be used for numerical treatment. This case is also divided into two cases, one is with high permeability rock matrix, and the other is with low permeability rock matrix. In the former case, τ_{pe} is short enough compared with τ_{hc}, so that complete porous medium assumption can be applied. In the latter case, τ_{pe} is comparable with or greater than τ_{hc}, so the effect of heat conduction appears depending on the matrix permeability k_m.

If τ_{pe} is greater than the time of interest, the pressures within the rock matrix cannot reach to equilibrium with fracture zone within the time. In this case, MINC method should be used to represent transient flow between rock matrix and fracture zone. In this case, however, if τ_{pe} is short enough compared with τ_{hc}, there is no heat conduction effect, and models with the same k_m/λ^2 (λ is the fracture spacing) behave the same way.

Using above classification of Pritchett and Garg(1990), judgement for choosing numerical method can be made quantitatively, considering the time of interest, compressibility (two-phase or single-phase), rock matrix permeability, and fracture spacing.

However, in the real geothermal application, existence of "global flow", which is not present in the above zero-dimensional model, makes reservoir behavior much more complicated. In this paper, numerical simulation studies to assess the influence of the global flow on the behavior of two-phase fractured reservoirs are discussed.

PRODUCTION INDUCED BOILING IN A RADIAL FLOW MODEL

Reservoir behavior associated with production and injection has a much shorter time scale compared with natural state problems, and sometimes it cannot be treated by a "porous medium" assumption. In many geothermal reservoirs, boiling of fluids occurs in formations near production wells, due to production induced pressure decrease. Two-phase fluid compressibility is larger than that of single phase fluid by three orders of magnitude, and it often makes τ_{pe} long enough to be comparable with τ_{hc}.

At first, we studied two-phase reservoir behavior using a radial flow model with production from a horizontal formation where fractures are distributed homogeneously. The parameters of the model are listed in Table 1. The initial condition of the reservoir is a saturated liquid at 300°C. Production calculations were performed for an interval of 10^7 seconds (4 months).

The fluid and heat flow between the fracture and country rock (matrix), and within the matrix region is controlled by the fracture spacing and matrix permeability. Here, we consider nine different cases of fractured reservoirs, by the combination of three different fracture spacings and three different matrix permeabilities. "Global" permeability and porosity for all cases are the same as those of the reference "porous medium" case.

Table 2 shows τ_{pe} and τ_{pc} for the nine cases. Within the calculation time of 10^7 seconds, all cases H, which have the highest matrix permeability, and all cases M, which have an intermediate matrix permeability, reach to the pressure equilibrium. On the other hand, case 10L, which has the lowest matrix permeability and the largest fracture spacing, cannot reach to the pressure equilibrium. For cases H, the heat conduction effect is slower than the pressure relaxation. For cases M, they have the same time scale. And for cases L, the heat conduction effect comes faster than the pressure relaxation.

Figure 1 shows numerical representation of the fractured reservoirs by MINC method. Numerical blocks which represent fractures are interconnected, and global flow can only passes through fracture blocks. Numerical blocks which represent matrix regions exchange heat and mass with the adjacent fracture blocks. The flow into the interior of matrix region is expressed by the connection of separated numerical blocks (shells).

The calculations were performed using the STAR general-purpose geothermal reservoir simulator (Pritchett, 1989). In the "MINC" medium representation on the sub-grid scale, the STAR simulator idealizes a "typical" block of matrix as a sphere, surrounded by a concentric spherical shell of high-permeability material representing the fracture zone. In the present calculations, the matrix region was subdivided into 6 concentric spherical shells for numerical purposes (for explanation of the MINC representation employed in the STAR code, see e.g. Pritchett and Garg, 1990).

Figure 2 shows the calculated pressure change in the well block. The pressure change of the "porous medium" case, which is shown as a straight line on the semi-log plot, represents the "global" permeability-thickness and storativity of the reservoir. For the "fractured reservoir" cases, the calculated results are largely affected by the matrix permeability, and also there are some differences in the pressure changes

Table 1. Model parameters used for the numerical simulation of a production test with in-situ boiling.

RESERVOIR GEOMETRY
- Horizontal layer : Thickness = 100 m
- Numerical blocks: divided by distance from the production well. Distance between the well center and block boundary = r(i); r(1)=0.1 m, $\Delta r(i+1) = \Delta r(i) \times 1.3$, r(max) = r(40) = 12,039 m

ROCK PROPERTIES
- (1) Common properties
  - Rock grain heat capacity = 1000 J/kg°C
  - Rock grain thermal conductivity = 2.5 W/m°C
  - Rock grain density = 2700 kg/m^3
- (2) Well block
  - Porous medium
  - Porosity = 0.99
  - Permeability = 10^{-10} m^2
- (3) Reservoir blocks (porous medium or fractured)
  - Total porosity = 0.05
  - Global permeability = 10^{-13} m^2
  - Fracture volume ratio to total volume = 0.1
  - Porosity of fracture = 0.1

INITIAL CONDITIONS
- Temperature: 300 °C
- Pressure: 8.5927 MPa (saturation pressure for 300°C)

PRODUCTION
- 31.416 kg/sec for 10^7 sec (about 4 month)

Table 2. Times (in seconds) required for pressure equilibrium (τ_{pe}) and temperature equilibrium (τ_{hc}) of the nine cases for numerical simulation of in-situ boiling.

fracture spacing (m) / rock matrix permeability (md)	1	$\sqrt{10}$	10
0.1	(1H) $\tau_{pe}=10^4$ $\tau_{hc}=10^5$	(3H) $\tau_{pe}=10^5$ $\tau_{hc}=10^6$	(10H) $\tau_{pe}=10^6$ $\tau_{hc}=10^7$
0.01	(1M) $\tau_{pe}=10^5$ $\tau_{hc}=10^5$	(3M) $\tau_{pe}=10^6$ $\tau_{hc}=10^6$	(10M) $\tau_{pe}=10^7$ $\tau_{hc}=10^7$
0.001	(1L) $\tau_{pe}=10^6$ $\tau_{hc}=10^5$	(3L) $\tau_{pe}=10^7$ $\tau_{hc}=10^6$	(10L) $\tau_{pe}=10^8$ $\tau_{hc}=10^7$

among cases of the same matrix permeability but of different fracture spacings.

For cases H, pressure equilibrium time is short compared with the calculation time, and the time scale for heat conduction effect is larger than the pressure equilibrium time by one order of magnitude. In these cases, the results had been expected to be the same as the "porous reservoir" case on the basis of the criterion proposed by Pritchett and Garg (1990). However, the calculated results for cases H (Figure 2) are different from the "porous reservoir" result. The pressures of cases H are larger at each time than the "porous" model, although the lines of pressure change are almost parallel to the "porous" result. This difference seems to be caused by the existence of "global" flow which is not present in the zero-dimensional model.

In order to understand the cause of this difference, we checked steam saturations of the fracture and the matrix regions. At 10^5 seconds (about one day) from the beginning of production, the steam saturation in the fracture of the numerical block next to the well block is 0.16. At this time, the steam saturation of the matrix is 0.65 for every shell. Although the pressure and temperature are in equilibrium, large difference of steam saturations between

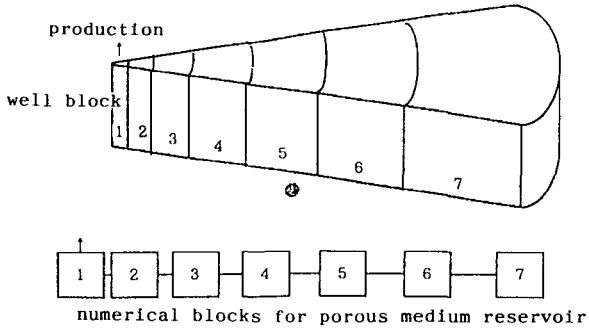

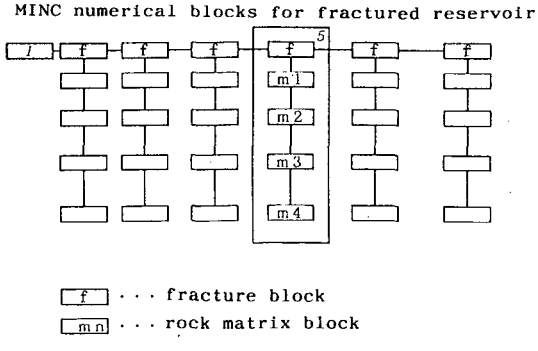

Fig. 1. Numerical block configurations for the production test. Fracture blocks are connected in the "MINC" model for global flow representation.

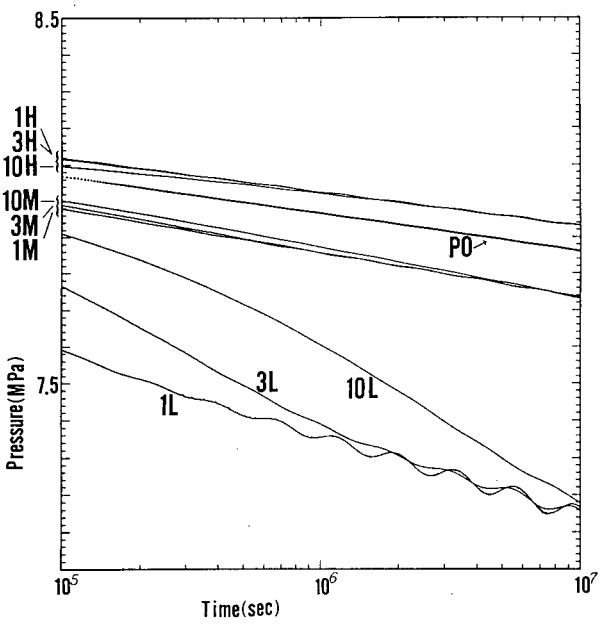

Fig. 2. Pressure transients of the well block in a production test with in-situ boiling. Results are shown for nine different fractured reservoir cases and a "porous" reservoir case.

the fracture and matrix exists. This is because the matrix region only supplies fluid to the fracture and becomes highly steam saturated, while the fracture gets fluid from the matrix and also from the global flow through fractures. These different steam saturations lead to different flow conditions through relative permeability difference.

In our numerical calculation, we used a X-type relative permeability function with residual saturations of water and steam of 0.3 and 0.05 respectively. On the basis of this function, the relative permeability of water is 0.77 and that of steam is 0.12 in the fracture, and these control global flow condition in the reservoir. On the other hand, the steam saturation in the same numerical block of the "porous medium" reservoir is 0.23. In this case, the relative permeabilities of water and steam are 0.67 and 0.19 respectively. Considering total mass flux for a constant pressure gradient, the global flow through the fracture zone will have a larger flux rate than the "porous medium" reservoir of the same global permeability. This higher mobility of cases H makes the pressure decrease smaller than the "porous" reservoir.

The pressure of case 10H is a little lower than cases 1H and 3H at early times. This is because only case 10H has not attained pressure equilibrium at these times.

Pressure decreases of all of cases M and L are larger than the "porous" case as seen in Figure 2. The time constant of temperature relaxation in the matrix region is shorter than the pressure time constant for cases L, and they are comparable for cases M. At time scales before reaching pressure equilibrium between the fracture and matrix, the temperature is lower in the fracture than in the matrix under the two-phase conditions. For cases L and M, rapid heat conduction takes place in these short time scales due to short τ_{hc}. This facilitates the increase in steam saturation in the fracture zone, leading to lower global flow mobility. As a consequence, the pressure decrease at the well block becomes larger than the "porous medium" case.

The time constant τ_{hc} is 10^6 seconds for cases 3L and 3M, and 10^7 seconds for cases 10L and 10M. As seen in Figure 2, after 10^6 (10^7) seconds of production , case 3L (10L), and case 3M (10M) behave as the same way as case 1L and case 1M respectively.

The pressure fluctuations of cases 1L and 3L seen in Figure 2 are caused by jumps of boiling front over finite distance corresponding to the size of numerical blocks, and has no physical meaning.

As we have mentioned above, the reservoir behavior with global flow is more complicated than that without global flow, mainly because of heterogeneous distribution of steam saturation between the fracture and matrix regions. The present result is thought to be useful when we analyze the complicated behaviors of production-induced boiling in fractured reservoirs.

PRODUCTION FROM A TWO-DIMENSIONAL GEOTHERMAL RESERVOIR

In this section, we use a mathematical reservoir model of one of geothermal fields in Japan for production simulation. However, allocations of production and injection wells, production rates, and production conditions including wellhead pressures used in this paper are all just hypothetical.

Figure 3 shows the computational grid blocks of the vertical two-dimensional reservoir model (thickness is 500m). High permeability (100 md) reservoir (A) is formed along a large fault zone, and

is covered by a low permeability caprock (D). Hot water is fed from the deep conduit (E) into the reservoir, and flow out through the horizontal conduit (B), surrounding rocks (C), and a permeable passage (F) through the caprock to the surface. In the permeable passage and in most of the upper part of the reservoir, a two-phase zone with high steam saturations is developed under the natural state conditions.

Three hypothetical production wells and several injection wells are set in the model as shown in the figure. Production calculations were done for 30 years. Constant steam flowrate to produce 10MW of electricity was assumed. A fixed separator pressure of 5 bars was used, and all separated liquid water and small amount of steam condensate were reinjected. For the calculations, the newest version of STAR geothermal reservoir simulator (Pritchett, 1993) was used.

A "porous" medium reservoir model (Case P) and two "MINC-type fractured reservoir" models (Case F30 and F100) were applied to the production calculation, using the same boundary conditions and geologic structures, and global permeabilities. The fracture spacing and matrix permeability are 30m and 0.001 md respectively in Case F30, and 100m and 0.01 md respectively in Case F100. (The matrix region was subdivided into 4 shells in both cases.) The time constant of pressure equilibrium, τ_{pe} is about 30 years under the two-phase conditions for both cases. Due to the difference of fracture spacings, they have different time constants of temperature equilibrium, τ_{he}. In Case F30, τ_{he} is about 3 years, and in Case F100, τ_{he} is about 30 years.

Figure 4 shows the total fluid production rate of the three cases. Since the steam flowrate is fixed, the total fluid production rate (water and steam) required by the power station will change with time, and is inversely correlated with the average produced fluid enthalpy (the steam saturation in the blocks of production feedpoints). Figure 5 shows the steam saturation in a block centrally located in the production zone. For the "fractured reservoir" cases, the steam saturations of the fracture and the center of matrix region are both shown. Figure 6 shows temperature changes of the same production block for the three cases. Since, in two-phase flow, fluid pressures and temperatures lie along the saturation curve for steam/water mixtures, the pressure changes of the production block can be seen from Figure 6.

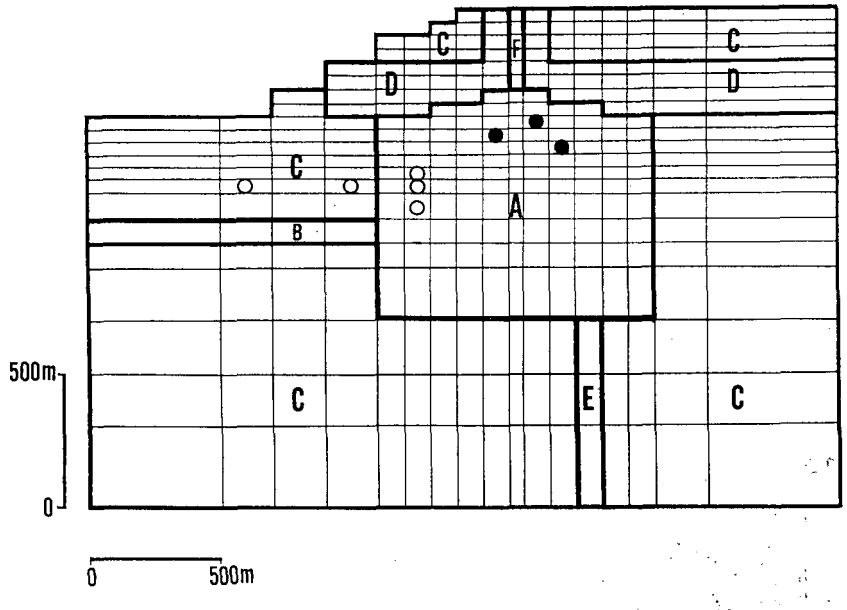

Fig. 3. Computational grid block used in the numerical simulation of production from a vertical two-dimensional geothermal reservoir model. Letters A to F represent geologic formations enclosed by bold lines. The symbol ● represents production feed points and the symbol ○ represents injection feed points.

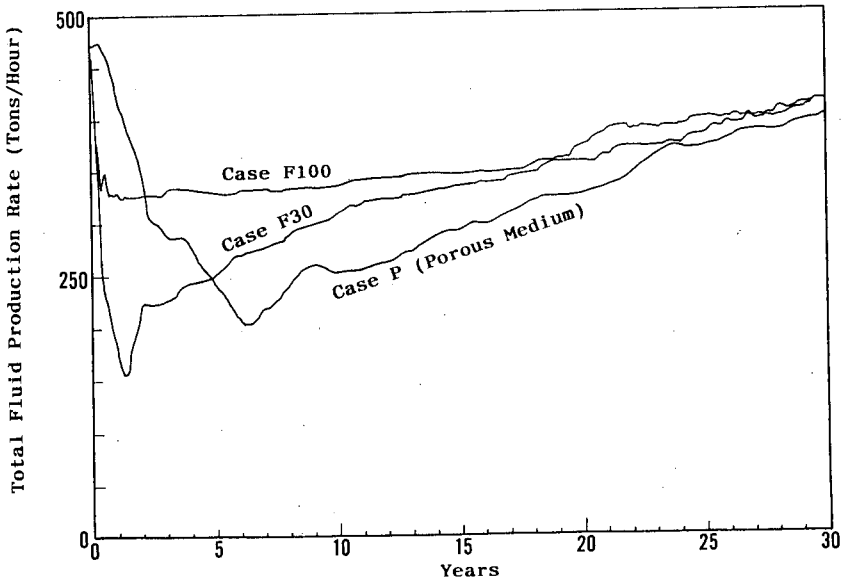

Fig. 4. Change in total fluid production rate versus time.

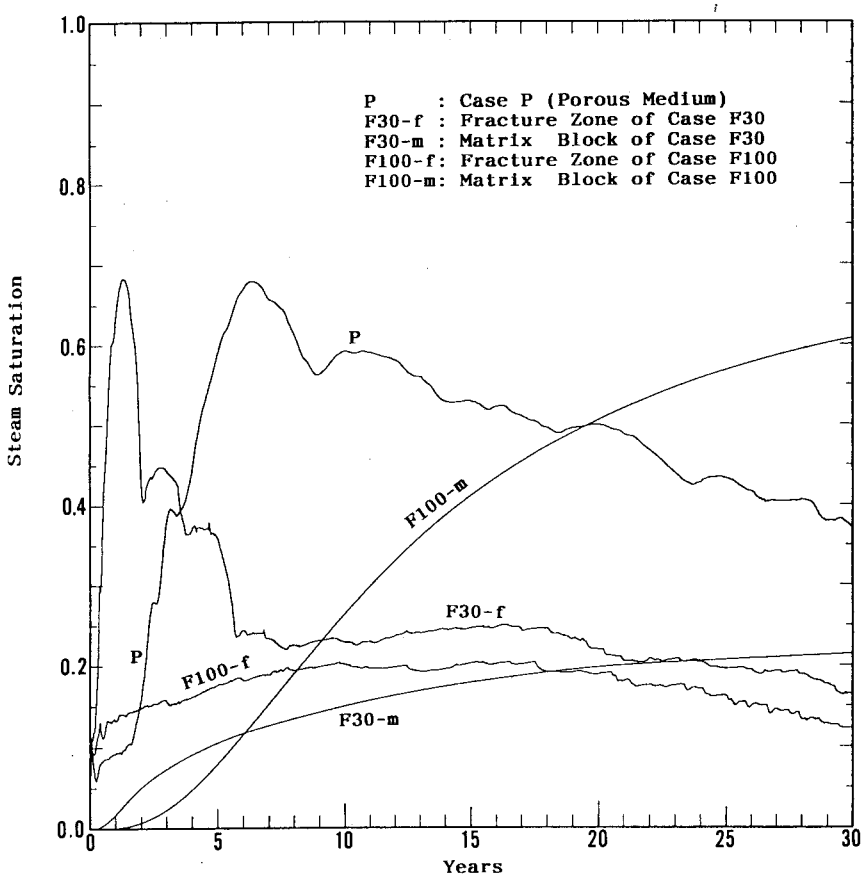

Fig. 5. Change in steam saturation versus time in the grid block of the middle elevation production feedpoint.

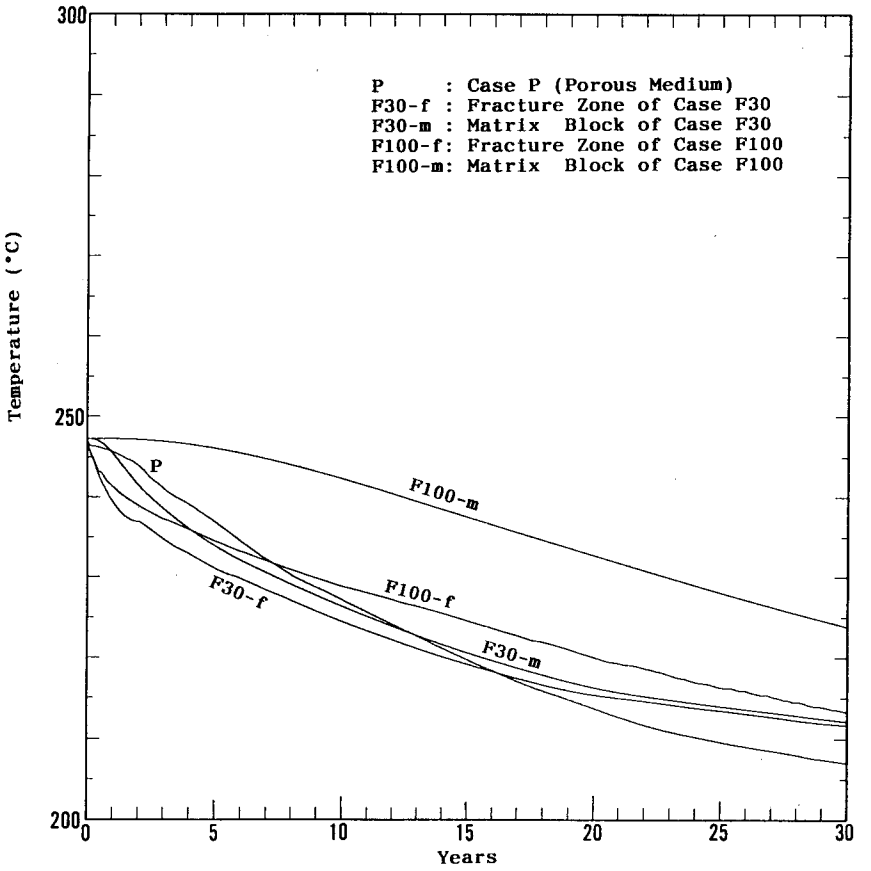

Fig. 6. Change in temperature versus time in the same grid block as Figure 5.

At early times (up to 1-2 years), the temperature (and pressure) decrease is larger for "fractured reservoir" cases than for "porous medium" case (Figure 6), even though the total production rate is lower for the "fractured reservoir" cases as seen in Figure 4. This behavior is consistent with the results for the "radial flow" model described in the previous section. Considering the relationship among τ_{pe}, τ_{hc} and the time of interest, Case F30 and F100 correspond to Case 3L and 10M in the previous section respectively. The same explanation as that described in the previous section can be applied to understand the early time behaviors of the "fractured reservoirs" shown in Figures 4 to 6. Due to the large τ_{pe}, the pressure in the fracture decreases faster than the "porous medium" case. The steam saturation in the fracture zone rises very quickly due to the rapid heat conduction effect for Case F30. This brings about reduction in the global flow mobility and facilitates the pressure decrease.

The histories of total fluid production rate at early times are largely different among the three cases considered here (Figure 4). It should be noted that rapid decrease in the total production rate is present at early stages for the fractured two-phase reservoirs.

After 1-2 years of operation, low-enthalpy fluid inflow from the reinjection zone is probably involved for "fractured reservoir" cases. The "cold front" travels faster with increasing fracture spacing, so the steam saturation in the fracture does not show any significant increase for Case F100 (100 m fracture spacing) as seen in Figure 5. In Case F30 (30 m fracture spacing), the influence of the low-enthalpy fluid starts to appear about 1.5 years and suppress the steam saturation in the fracture.

REFERENCES

Pritchett, J. W. (1989) Star user's manual. S-Cubed Report SSS-TR-89-10242.

Pritchett, J. W. and Garg, S. K. (1990) On similitude, heat conduction, and two-

phase flow in fractured porous media. Proc. Fifteenth Workshop on Geothermal Reservoir Engineering, Stanford University.

Pritchett, J. W. (1993) Star user's manual. S-Cubed Report SSS-TR-92-13366.

Pruess, K. and Narasimhan, T. N. (1985) A practical method for modeling fluid and heat flow in fractured porous media. SPE Journal, Feb., 14-26.